

Electronic Supplementary Information

**Heteropoly acid-grafted iron oxide catalysts for efficient selective
catalytic reduction of NO_x with NH₃**

Yang Geng ^{a*}, Zhihua Lian ^b, Yan Zhang ^{b,c}, Janqi Liu ^{b,c}, Dongliang Jin ^d, Wenpo Shan ^{b,c*}

^a School of Environment Engineering, Wuxi University, Wuxi 214105, P. R. China

^b Center for Excellence in Regional Atmospheric Environment and Key Laboratory of Urban Pollutant Conversion, Institute of Urban Environment, Chinese Academy of Science, Xiamen 361021, P. R. China

^c Zhejiang Key Laboratory of Urban Environmental Processes and Pollution Control, Ningbo Urban Environment Observation and Research Station, Institute of Urban Environment, Chinese Academy of Sciences, Ningbo 315800, P. R. China

^d School of Environmental Science and Engineering, Nanjing University of Information Science & Technology, Nanjing 210044, P. R. China

*Corresponding author: gengy@cw Xu.edu.cn (Yang Geng); wps Shan@iue.ac.cn (Wenpo Shan)

S1 NO oxidation

Fig. S1 shows the NO conversion during the NO oxidation experiment over HSiW/Fe₂O₃, HPW/Fe₂O₃, and HPMo/Fe₂O₃ catalysts at 150-500 °C. The NO conversion over all catalysts was below 9% at the whole temperature window. It was observed that the NO oxidation activity on HPMo/Fe₂O₃ was less than those on HSiW/Fe₂O₃ and HPW/Fe₂O₃ catalysts at 250-500 °C. With the increase of temperature, both HSiW/Fe₂O₃ and HPW/Fe₂O₃ catalysts could reach the maximum values of NO conversion at 300 °C.

S2 XPS results of W 4f and Mo 3d

The XPS results of W 4f and Mo 3d of HPA/Fe₂O₃ catalysts are shown in Fig. S2. A doublet peak corresponding to W 4f photoelectrons appeared at 37.7-37.5 eV and 35.6-35.4 eV were obtained on the HSiW/Fe₂O₃ and HPW/Fe₂O₃. This was associated with W in the formal (VI) oxidation state. The Mo 3d binding energies of HPMo/Fe₂O₃ mainly centered at 236.0 and 232.8 eV, which were attributed to Mo⁶⁺.

S3 DFT calculations

S3.1 Computational Methods

All calculations are based on the CASTEP program package, using the generalized gradient approximation (GGA-PBE) with the Perdew-Burke-Ernzerh of exchange correlation function and super soft pseudopotential, and using a plane wave extension with a cut-off energy of 500 eV. The Brillouin area sampling adopts the Monkhorst-Park format, and the model adopts a $1 \times 1 \times 1$ K-point grid. The convergence standards for structure optimization and energy calculation are SCF tolerance is 1.0×10^{-5} eV/atom, Energy tolerance is 1.0×10^{-5} eV/atom, Max force tolerance is 0.05 eV/Å, and Maximum displacement tolerance is 0.002 Å.

S3.2 Formation of NH₂NO

The formation of NH₂NO is a key step in the SCR reaction.^{S1} NH₂NO undergoes a series of reactions and decomposes into N₂ and H₂O.^{S2-3} DFT calculations were utilized to further investigate the Langmuir-Hinshelwood mechanism and the Eley-Rideal mechanism of the SCR reaction over HPW/Fe₂O₃. As shown in Fig. S5A, the reaction energy of NH₂NO formation on HPW/Fe₂O₃ through the Langmuir-Hinshelwood mechanism was 0.85 eV. However, when NH₂NO formed on

HPW/Fe₂O₃ through the Eley-Rideal mechanism, the reaction energy was -0.33 eV (shown in Fig. S5B). The calculation results suggested that the NH₂NO formation is more inclined to the SCR reaction pathway of the Eley-Rideal mechanism.

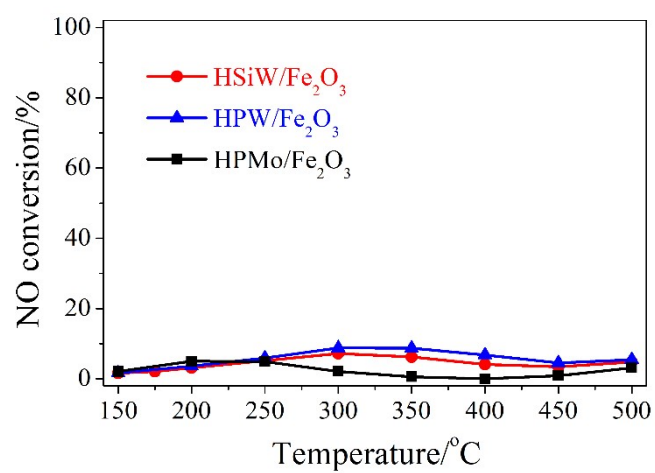


Fig. S1. NO oxidation over HSiW/Fe₂O₃, HPW/Fe₂O₃, and HPMo/Fe₂O₃ catalysts. Reaction conditions: [NO] = 500 ppm, [O₂] = 5%, catalyst mass = 100 mg, total flow rate = 100 mL min⁻¹, and WHSV = 60,000 cm³ g⁻¹ h⁻¹.

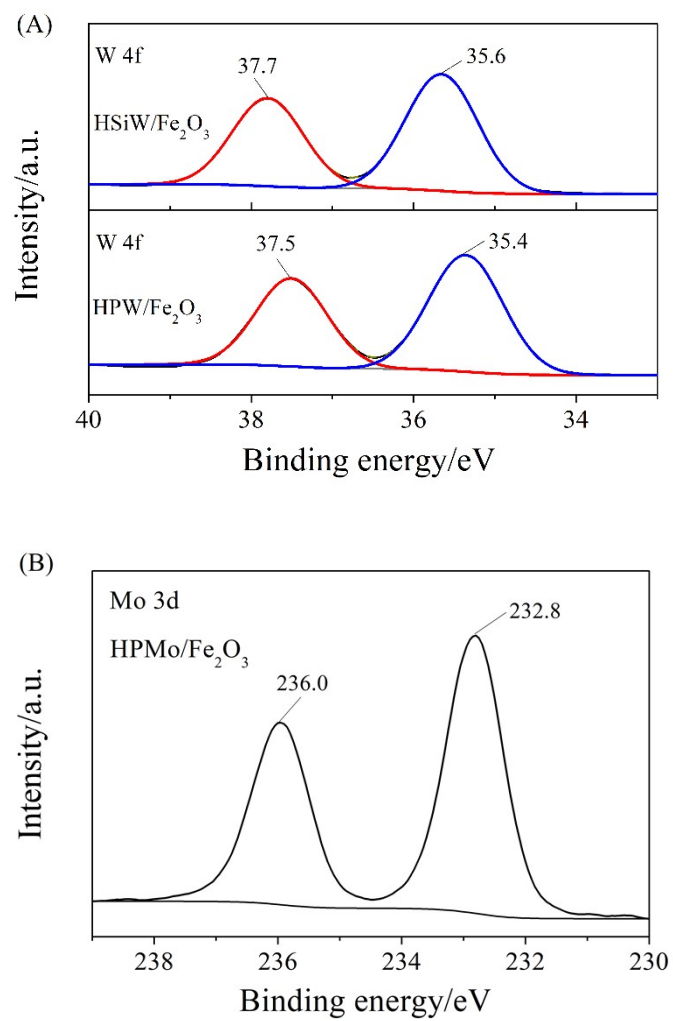


Fig. S2. XPS spectra of HSiW/Fe₂O₃, HPW/Fe₂O₃, and HPMo/Fe₂O₃ catalysts over the spectral regions of W 4f and Mo 3d.

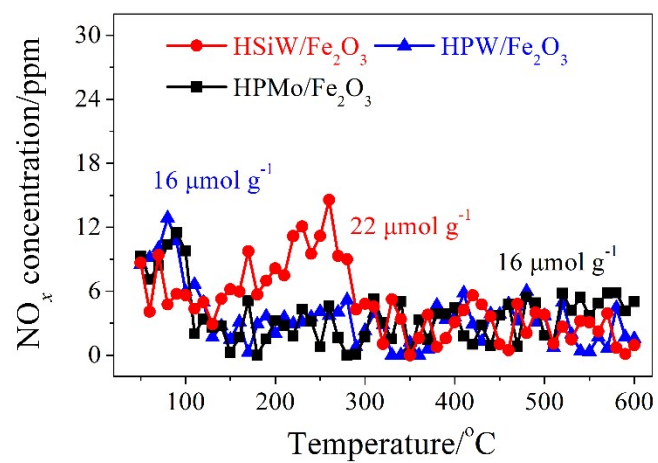


Fig. S3. NO_x-TPD results for HSiW/Fe₂O₃, HPW/Fe₂O₃, and HPMo/Fe₂O₃ catalysts.

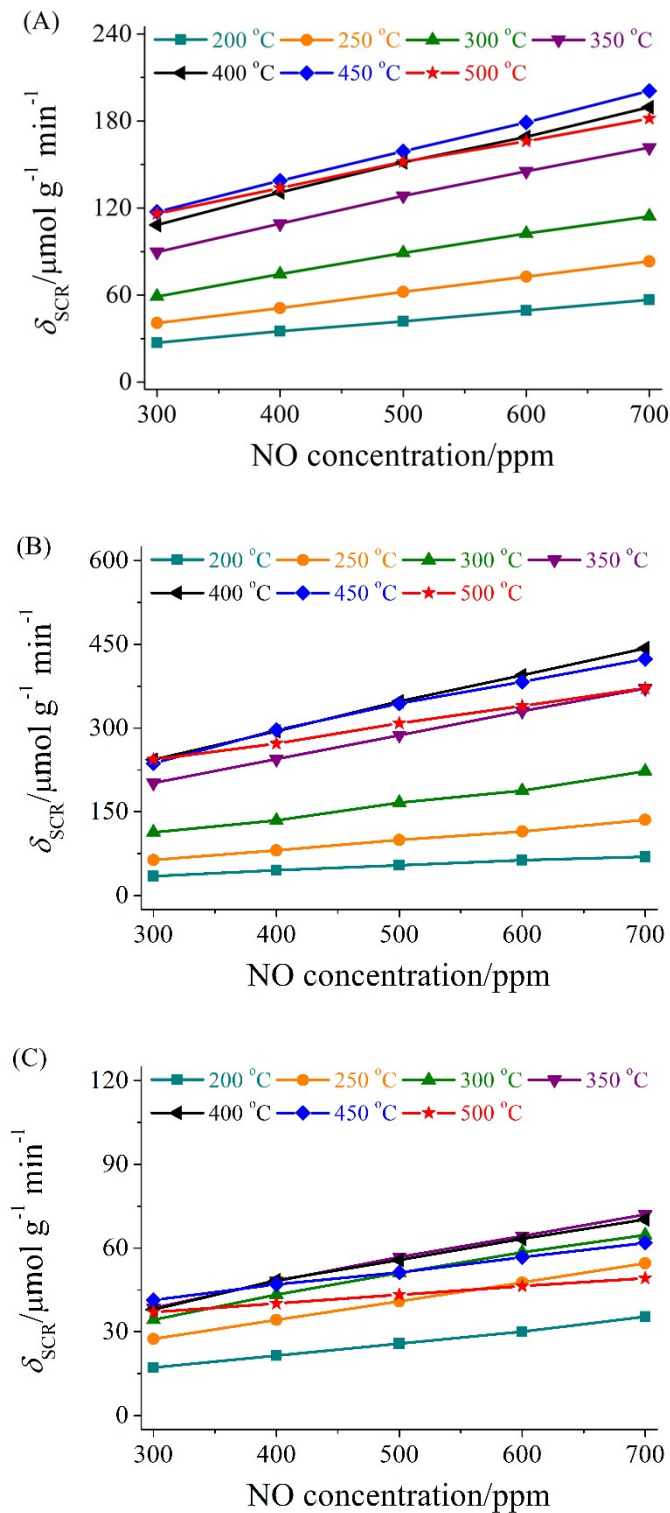


Fig. S4. Dependences of the SCR reaction rate during NO reduction over (A) HSiW/Fe₂O₃, (B) HPW/Fe₂O₃, and (C) HPMo/Fe₂O₃ on gaseous NO concentration. Reaction conditions: [NH₃]=500 ppm, [NO]=300-700 ppm, [O₂]=5%, catalyst mass=3-30 mg, total flow rate=400 mL min⁻¹, and WHSV=800,000-8,000,000 cm³ g⁻¹ h⁻¹.

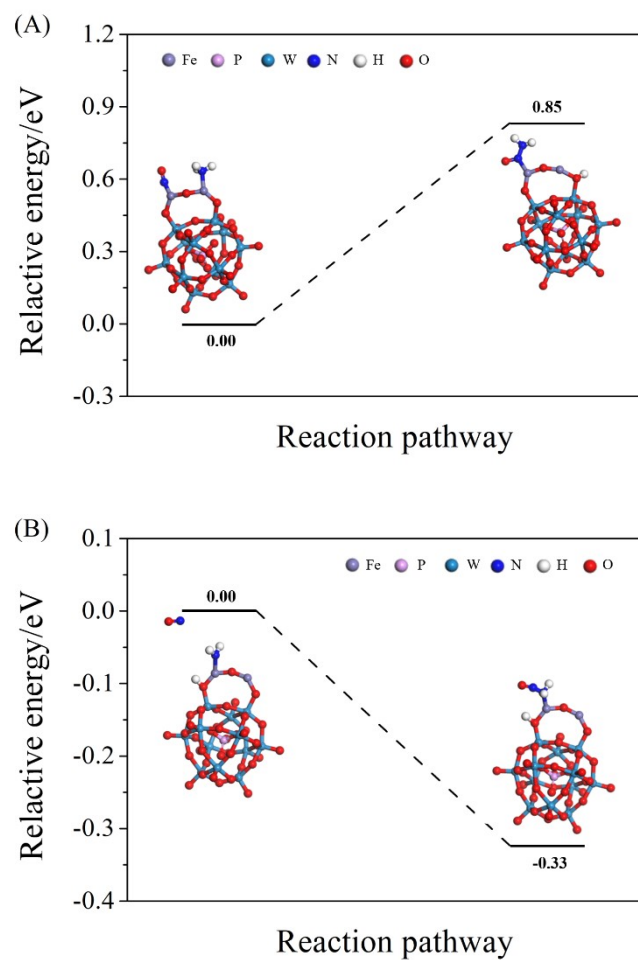


Fig. S5. Energy profiles and the corresponding optimized structures of the NH_2NO formation on $\text{HPW}/\text{Fe}_2\text{O}_3$ through (A) the Langmuir-Hinshelwood mechanism and (B) the Eley-Rideal mechanism.

References

- S1 J. Q. Liu, X. Ren, Z. D. Zhang, N. Sun, H. L. Tan and J. M. Cai, *J. Phys. Chem. C*, 2021, **125**, 14228-14238.
- S2 G. Z. Qin, Y. N. Zhang, J. F. Zheng, Y. F. Li, X. J. Han and Z. G. Huang, *Fuel*, 2023, **349**, 128621.
- S3 D. D. Ren, K. T. Gui, S. C. Gu and Y. L. Wei, *Appl. Surf. Sci.*, 2020, **509**, 144659.